A NUMERICAL METHOD FOR MASONRY VAULTS

Internal Report C95-25

19 Luglio 1995

M. Lucchesi
C. Padovani
G. Pasquinelli
N. Zani

A NUMERICAL METHOD FOR MASONRY VAULTS

M. LUCCHESI[1] C. PADOVANI[2] G. PASQUINELLI[2] N. ZANI[2]

1. *Università di Chieti, viale Pindaro 42, 65100 Pescara*
2. *CNUCE-CNR, via Santa Maria 36, 56100 Pisa*

CNUCE Internal Report C95-25

Abstract
A method for studying masonry vaults with the aim of furnishing a useful computational tool both for evaluating the safety of masonry monuments and guiding the choice of restoration operations is presented. The maximum modulus eccentricities surface playing a role analogous to that of line of thrust for arches is defined; subsequently a spherical vault subjected to its own weight and a point load at the crown is analyzed and the maximum modulus eccentricities surface in correspondence of the collapse is explicitly calculated. Finally the baptistery of Volterra cathedral is studied, in particular the effectiveness of the existing reinforcement is checked.

1. INTRODUCTION

A numerical method for solving plane equilibrium problems of masonry solids has been proposed in a previous work [1]. The masonry is considered to be a non-linear elastic material characterised by the constitutive hypothesis that the total strain $\mathbf{E}$ is the sum of an elastic part $\mathbf{E}^e$ and an inelastic part $\mathbf{E}^a$, positive semi-definite, $\mathbf{E} = \mathbf{E}^e + \mathbf{E}^a$. Moreover, the stress $\mathbf{T}$, negative semi-definite and orthogonal to $\mathbf{E}^a$, depends linearly and isotropically on $\mathbf{E}^e$: thus, $\mathbf{T} = 2\mu\mathbf{E}^e + \lambda\ \mathrm{tr}(\mathbf{E}^e)\mathbf{I}$, with μ and λ the Lamé moduli of the material. $\mathbf{E}^a$ is sometimes called the fracture strain because the body can be expected to crack in the regions where $\mathbf{E}^a$ is different from zero.

The solution to equilibrium problems by the finite element method is arrived at by means of the Newton-Raphson method, which requires explicit calculation of the derivative of stress with respect to the total strain .

In [2] and [3] the method was extended to enable, among other enhancements, solution of three-dimensional problems, and has been successfully applied to the study of masonry structures in proximity to collapse as well. In particular, calculations of the lines of thrust from the stress field determined by finite element analysis has proven to be particularly useful in the evaluation of the safety of arches and the effectiveness which can be expected of any restoration and/or reinforcement work.

In this paper we intend to propose a method for studying masonry vaults with the aim of furnishing a useful computational tool both for evaluating the safety of masonry monuments and guiding the choice of restoration operations.

Firstly, in Section 2 a surface called the *maximum modulus eccentricities surface* (m.m.e.s.) is defined and several important properties which it possess are proven. In masonry vaults the m.m.e.s. plays a role analogous to that of line of thrust for arches.

Section 3 deals with a circular plate subjected to progressively increasing loads until collapse is reached. The m.m.e.s. is then determined from the numerically calculated stress field. Once this surface is known the mechanism of collapse can be predicted, and some simple formulas for calculating the collapse load can be formulated.

Section 4 is dedicated to the study of spherical vaults subjected to their own weight and a point load at the crown. The finite element analysis confirms that the vault collapses by an "orange-

slices" mechanism and by virtue of the hypothesis that the circumferential normal force and bending moment are null, the stress characteristics and the m.m.e.s. are explicitly determined. The values of the m.m.e.s. turn out to be in a good agreement with those calculated numerically.

Finally, in Section 5 the baptistery in Volterra, dating back to the X C. and currently under restoration, is analyzed. In particular, the stress field is determined and the effectiveness of the existing reinforcement - two chains for the vault and one for the baptistery walls - is checked.

The numerical results presented in this paper have been obtained by using the techniques proposed in [1], [2] and [3] and implemented in the finite element code NOSA [4]; in particular we have used a non-conforming eight-node shell element whose formulation is based on the Love-Kirchhoff hypothesis [5].

2. THE MAXIMUM MODULUS ECCENTRICITIES SURFACE

The principles of limit analysis of masonry arches are based on three assumptions: that the material is non-resistant to traction, has infinite compressive strength and that the voussoirs do not slide with respect to each other [6].

From the first hypothesis it follows simply that the line of thrust must be entirely contained within the arch in order to meet equilibrium conditions. Moreover, if a point exists where the line of thrust intersects the boundary of the arch, that point constitutes a hinge. Therefore, when at least four hinges whose positions alternate from intrados to extrados, are present, the structure is labile. Since by virtue of the third hypothesis this is the only kinematically admissible mechanism the existence of a line of thrust equilibrated and entirely contained within the arch also suffices to guarantee stability.

Here our purpose is to extend these concepts to masonry vaults and apply them with the help of the numerical techniques recalled in Section 1. To this end, we define a surface, called the *maximum modulus eccentricities surface,* which for masonry vaults plays a role analogous to that of pressure curves for arches.

Let us consider the vault element with thickness h shown in Figure 1; let η_1, η_2 be an orthogonal coordinate system, not the necessarily principal one, defined on the mean surface with ζ as the coordinate in the normal direction **n**. For each point having coordinates (η_1, η_2, ζ), and for each unit vector $\mathbf{g}_\alpha = (\cos\alpha, \sin\alpha)$ in the plane tangent to the mean surface, where $\alpha \in (-\pi/2, \pi/2]$ is the angle formed by $\mathbf{g}_\alpha$ with direction η_1 in the counterclockwise direction, let us put

$$\sigma_\alpha(\eta_1, \eta_2, \zeta) = \mathbf{g}_\alpha(\eta_1, \eta_2) \cdot \mathbf{T}(\eta_1, \eta_2, \zeta)\, \mathbf{g}_\alpha(\eta_1, \eta_2)\ ; \tag{2.1}$$

where $\mathbf{T}(\eta_1, \eta_2, \zeta)$ is the stress tensor. Thus, the relations

$$N(\eta_1, \eta_2; \alpha) = \int_{-h/2}^{h/2} \sigma_\alpha(\eta_1, \eta_2, \zeta)\, d\zeta, \quad M(\eta_1, \eta_2; \alpha) = \int_{-h/2}^{h/2} \sigma_\alpha(\eta_1, \eta_2, \zeta)\, \zeta\, d\zeta \tag{2.2}$$

define the normal force and bending moment corresponding to $\mathbf{g}_\alpha$. In view of the fact that $\mathbf{T}$ is negative semi-definite, $N(\eta_1, \eta_2; \alpha)$ is non-positive for every α.

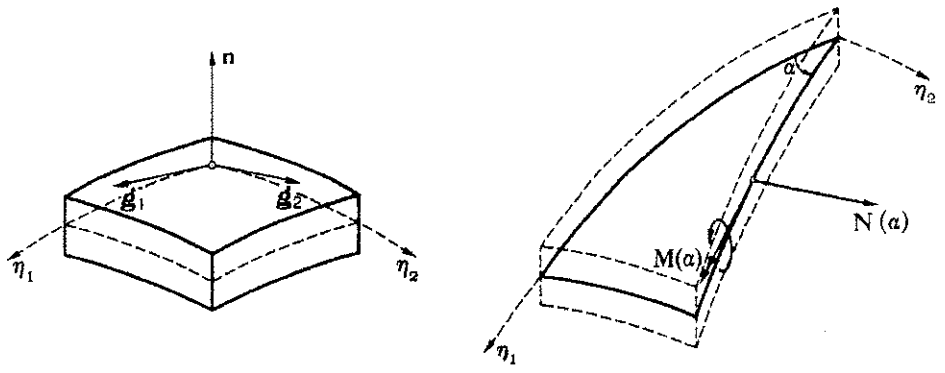

Figure 1. Coordinates on the mean surface and stress characteristics.

Setting the point on the mean surface of the vault with coordinates (η_1, η_2) and placing for each $\zeta \in [-h/2, h/2]$ [1]

$$\mathbf{T}(\zeta) = \begin{bmatrix} \sigma_1(\zeta) & \tau(\zeta) \\ \tau(\zeta) & \sigma_2(\zeta) \end{bmatrix}, \tag{2.3}$$

from (2.1) the relation

$$\sigma_\alpha(\zeta) = \sigma_1(\zeta)\cos^2\alpha + \sigma_2(\zeta)\sin^2\alpha + 2\tau(\zeta)\sin\alpha\cos\alpha, \tag{2.4}$$

follows for each $\alpha \in (-\pi/2, \pi/2]$. Taking into account equation $(2.2)_1$, we then obtain

$$N(\alpha) = N_1\cos^2\alpha + N_2\sin^2\alpha + N_{12}\sin 2\alpha, \tag{2.5}$$

where

$$N_1 = \int_{-h/2}^{h/2} \sigma_1(\zeta)d\zeta, \qquad N_2 = \int_{-h/2}^{h/2} \sigma_2(\zeta)d\zeta, \qquad N_{12} = \int_{-h/2}^{h/2} \tau(\zeta)d\zeta. \tag{2.6}$$

Analogously, setting

[1] In the following the dependence of T, σ_α, N and M on (η_1,η_2) is omitted.

$$M_1 = \int_{-h/2}^{h/2} \sigma_1(\zeta)\,\zeta d\zeta\,, \quad M_2 = \int_{-h/2}^{h/2} \sigma_2(\zeta)\,\zeta d\zeta\,, \quad M_{12} = \int_{-h/2}^{h/2} \tau(\zeta)\,\zeta d\zeta\,, \tag{2.7}$$

in view of $(2.2)_2$, we have

$$M(\alpha) = M_1 \cos^2\alpha + M_2 \sin^2\alpha + M_{12} \sin 2\alpha\,. \tag{2.8}$$

In the following we constantly exclude that in some point of the vault the normal force is nil in all directions, namely that the equalities

$$N_1 = N_2 = N_{12} = 0 \tag{2.9}$$

hold. From this assumption it follows that there is at most one $\alpha \in (-\pi/2, \pi/2]$ such that $N(\alpha) = 0$. In order to check this result it is enough to consider that, in view of (2.5), $N(\pi/2) = N_2$ and $N(\alpha) = \cos^2\alpha(N_2\tan^2\alpha + 2N_{12}\tan\alpha + N_1)$ for $\alpha \neq \pi/2$ and that the non-positiveness of $N(\alpha)$ implies the inequality $(N_{12})^2 - N_1N_2 \leq 0$.

For $\alpha \in (-\pi/2, \pi/2]$, let

$$e(\alpha) = \frac{M(\alpha)}{N(\alpha)} = \frac{M_1\cos^2\alpha + M_2\sin^2\alpha + M_{12}\sin 2\alpha}{N_1\cos^2\alpha + N_2\sin^2\alpha + N_{12}\sin 2\alpha} \tag{2.10}$$

be the eccentricity corresponding to direction α. Function $e(\alpha)$ is well-defined and continuous for each $\alpha \in (-\pi/2, \pi/2]$, such that $N(\alpha) \neq 0$. We want to prove that even when there exists $\alpha' \in (-\pi/2, \pi/2]$, such that $N(\alpha') = 0$, $e(\alpha)$ can be extended continuously to α' and that its extension is therefore well-defined and continuous in the interval $(-\pi/2, \pi/2]$. To this end, we shall prove that if there exits $\alpha' \in (-\pi/2, \pi/2]$, such that $N(\alpha') = 0$, then $e(\alpha)$ is a constant function.

Firstly, let us observe that, by virtue of $(2.2)_1$ and the negative semi-definiteness of $\mathbf{T}$, $N(\alpha') = 0$ implies

$$\sigma_{\alpha'}(\zeta) = 0, \quad \text{for all } \zeta \in [-h/2, h/2]. \tag{2.11}$$

Therefore, in place of (2.1) we can write

$$\mathbf{g}_{\alpha'} \cdot \mathbf{T}(\zeta)\,\mathbf{g}_{\alpha'} = 0\,, \quad \text{for all } \zeta \in [-h/2, h/2]\,, \tag{2.12}$$

which, again in view of the negative semi-definiteness of $\mathbf{T}$, implies

$$\mathbf{T}(\zeta)\,\mathbf{g}_{\alpha'} = 0\,, \quad \text{for all } \zeta \in [-h/2, h/2]\,, \tag{2.13}$$

from which we obtain

$$\sigma_1(\zeta)\,\sigma_2(\zeta) - \tau(\zeta)^2 = 0\,, \quad \text{for all } \zeta \in [-h/2,\, h/2]\,. \tag{2.14}$$

If $\alpha' = \pi/2$, from (2.6) and (2.14) we obtain $\sigma_2(\zeta) = \tau(\zeta) = 0$, for each $\zeta \in [-h/2,\, h/2]$ and then, owing to (2.6), (2.7) and (2.10), we have $e(\alpha) = \dfrac{M_1}{N_1}$, for each $\alpha \in (-\pi/2,\, \pi/2]$.

Let us now suppose that $\alpha' \neq \pi/2$, and set $t' = \tan\alpha'$. From (2.4) and (2.11) we deduce

$$\sigma_1(\zeta) + \sigma_2(\zeta)(t')^2 + 2\tau(\zeta)t' = 0, \quad \text{for all } \zeta \in [-h/2,\, h/2] \tag{2.15}$$

and then, in view of (2.14), we can write

$$(t'\sigma_2(\zeta) + \tau(\zeta))^2 = 0\,, \quad \text{for all } \zeta \in [-h/2,\, h/2]\,. \tag{2.16}$$

Then, placing $\tau(\zeta) = -\,t'\sigma_2(\zeta)$, with the help of (2.4) and (2.14) we obtain

$$\sigma_\alpha(\zeta) = \sigma_2(\zeta)\,(\sin\alpha - t'\cos\alpha)^2\,. \tag{2.17}$$

Now the desired result follows from (2.2), (2.10) and (2.17).

It is interesting to note that if there exists α', such that $N(\alpha') = 0$, then $|N(\alpha)|$ reaches its maximum value in the direction orthogonal to α', as can be easily derived from relation (2.17).

For each point (η_1, η_2) of the mean surface, let $\alpha_0 \in (-\pi/2,\, \pi/2]$ be the value of α, not necessarily unique, for which function $|e(\alpha)| = \dfrac{|M(\alpha)|}{|N(\alpha)|}$ reaches its maximum value[2]. The quantity

$$\tilde{e}(\eta_1, \eta_2) = \frac{M(\alpha_0)}{N(\alpha_0)} \tag{2.18}$$

shall be called the *maximum modulus eccentricity* at point (η_1, η_2). The maximum modulus eccentricities surface (m.m.e.s.) is then the set of all points with coordinates $(\eta_1, \eta_2, \tilde{e}(\eta_1,\eta_2))$. Where two values α_0 and α_1 exist which maximize the function $\dfrac{|M(\alpha)|}{|N(\alpha)|}$ with $\dfrac{M(\alpha_0)}{N(\alpha_0)} = -\,\dfrac{M(\alpha_1)}{N(\alpha_1)}$, the m.m.e.s. is not defined.

It is important to point out that, in analogy to what occurs for the line of thrust in the case of arches, the m.m.e.s. corresponding to a negative semi-definite stress field is entirely contained within the vault. In fact, we can write

[2] The existence of the maximum is guaranteed by the fact that, as $e(-\pi/2) = e(\pi/2)$, function $|e(\alpha)|$ is continuous in the bounded and closed interval $[-\pi/2, \pi/2]$.

$$|M(\alpha_0)| = \left|\int_{-h/2}^{h/2} \sigma_{\alpha_0}(\zeta)\zeta d\zeta\right| \leq \int_{-h/2}^{h/2} |\sigma_{\alpha_0}(\zeta)\zeta| d\zeta \leq \frac{h}{2}\int_{-h/2}^{h/2} |\sigma_{\alpha_0}(\zeta)| d\zeta =$$

$$= \left|\frac{h}{2}\int_{-h/2}^{h/2} \sigma_{\alpha_0}(\zeta) d\zeta\right| = \frac{h}{2}|N(\alpha_0)| , \qquad (2.19)$$

where the next to last step is justified by the fact that, in view of (2.1), we have $\sigma_{\alpha_0}(\zeta) \leq 0$ for each ζ. The desired result follows from (2.18) and (2.19).

In view of (2.19), if the m.m.e.s. is tangent to the extrados or intrados along a path, this last can be considered the site of cylindrical hinges. The corresponding rotational axis coincides with the direction orthogonal to that for which the modulus of the eccentricity is maximum. Therefore, by generalizing accepted practice for arches [6], it seems natural to admit that vault collapse occurs when the m.m.e.s. is tangent to the extrados and intrados along paths so as to determine a hinge distribution sufficient to render the vault labile.

In order to determine the maximum and minimum points of function $e(\alpha)$, let us calculate the values of $\alpha \in (-\pi/2, \pi/2)$ for which $e'(\alpha)$, the derivative of e with respect to α is nil.

Denoting $n(\alpha)$ as the numerator of $e'(\alpha)$, from (2.10) we obtain

$$n(\alpha) = \{(M_2 - M_1)\sin 2\alpha + 2M_{12}\cos 2\alpha\}\,(N_1\cos^2\alpha + N_2\sin^2\alpha + N_{12}\sin 2\alpha) +$$

$$- \{(N_2 - N_1)\sin 2\alpha + 2N_{12}\cos 2\alpha\}\,(M_1\cos^2\alpha + M_2\sin^2\alpha + M_{12}\sin 2\alpha) . \qquad (2.20)$$

Putting $t = \tan\alpha$, by direct calculation we obtain

$$n(\alpha) = 2\cos^4\alpha\,(t^2 + 1)(at^2 + bt + c) , \qquad (2.21)$$

where

$$a = N_{12}M_2 - N_2M_{12} , \quad b = N_1M_2 - N_2M_1 , \quad c = N_1M_{12} - N_{12}M_1 . \qquad (2.22)$$

Thus, for $\alpha \in (-\pi/2, \pi/2)$, we have $e'(\alpha) = 0$, if and only if

$$a\sin^2\alpha + b\sin\alpha\cos\alpha + c\cos^2\alpha = 0 \qquad (2.23)$$

holds. It is easily verified that, if both a and b are nil, so is c, and that $e(\alpha)$ is constant, as is to be expected considering that $e(\pi/2) = e(-\pi/2)$. If $a = 0$ e $b \neq 0$, we have

$$e'(\alpha) = 0\,, \qquad \text{for } \alpha = \arctan\left(-\frac{c}{b}\right)\,. \tag{2.24}$$

In the general case for which $a \neq 0$, the values of α where $e'(\alpha)$ becomes zero are all and only those for which $\alpha = \arctan(z)$, with z, the root of the polynomial $p(z) = a\,z^2 + b\,z + c$. Let us suppose for the sake of simplicity that the reference system (η_1, η_2) is chosen so that $N_{12} = 0$. Therefore, from (2.22), taking into account that N_1 and N_2 are both non-positive, we obtain

$$\delta = b^2 - 4ac = (N_1 M_2 - N_2 M_1)^2 + 4(M_{12})^2\, N_1 N_2 \geq 0\,. \tag{2.25}$$

Therefore, the values of α we are looking for are

$$\alpha = \arctan\left(\frac{-\,b \pm \sqrt{\delta}}{2\,a}\right)\,. \tag{2.26}$$

In the particular case, frequently encountered in applications, in which the geometry of the vault and the loads have axial symmetry, the foregoing can be simplified. In fact, if as usual we choose coordinates (η_1, η_2) along the parallels and meridians, we have $N_{12} = 0$ and $M_{12} = 0$. Thus, in this case it follows from (2.22) that $a = c = 0$, and that function $e(\alpha)$, if not constant, has a relative extreme at $\alpha = 0$ and $\alpha = \pi/2$; so the eccentricity can reach its maximum modulus only in the direction of parallels and meridians.

3. THE CIRCULAR PLATE

In the cylindrical reference system $\{O, r, \theta, z\}$, let us consider the circular plate with radius R and thickness h,

$$\mathcal{P} = \{(r, \theta, z) \mid 0 \leq r \leq R,\ 0 \leq \theta < 2\pi,\ -\tfrac{1}{2}h \leq z \leq \tfrac{1}{2}h\},$$

constrained along the lateral surface $\{r = R\}$ in such a way that only rotations and vertical displacements are prevented (Figure 2). The plate is subjected to a vertical pressure p, uniformly distributed on the circle of the extrados $\{0 \leq r \leq b,\ 0 \leq \theta < 2\pi,\ z = -\tfrac{1}{2}h\}$ and a horizontal pressure q, uniformly distributed on the lateral surface. For the sake of simplicity, we have ignored weight, but the corresponding generalization presents no difficulties.

A quarter plate, with R = .5 m and h = .01 m, has been discretized and analyzed through the finite element code NOSA. After applying the horizontal pressure $q = 5.\ 10^4\ N/m^2$, the vertical pressure p, uniformly distributed throughout the extrados (b = R), is progressively increased by assigning successive load increments until convergence can be reached.

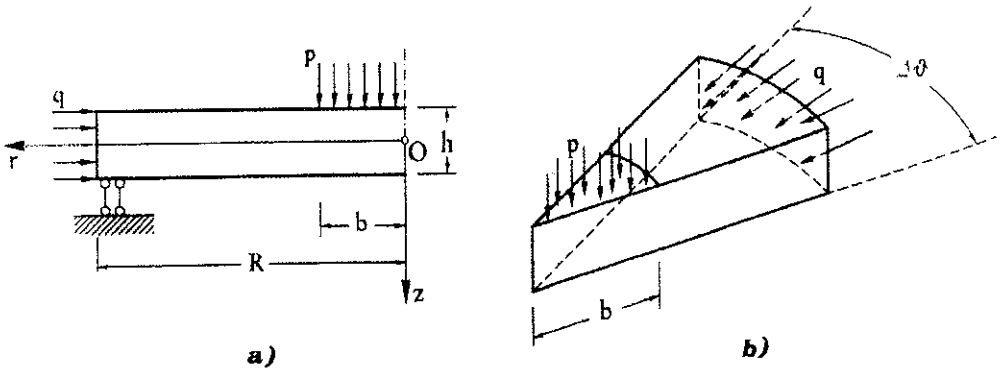

Figure 2. The circular plate.

Starting from the numerically calculated stress field corresponding to the last load increment, the m.m.e.s. shown in Figure 3 has been determined. Here the thickness of the plate has been magnified ten times in order to better illustrate the m.m.e.s. This last is a plane region coinciding with the extrados for $0 \leq r < R$, and discontinuous for $r = R$. In fact, for $0 \leq r < R$ the eccentricity e_θ corresponding to the circumferential direction is $-\frac{1}{2}h$, and that for the radial one e_r is, in absolut value, less than $\frac{1}{2}h$. On the contrary, for $r = R$ we have $e_\theta = -\frac{1}{2}h$ and $e_r = \frac{1}{2}h$.

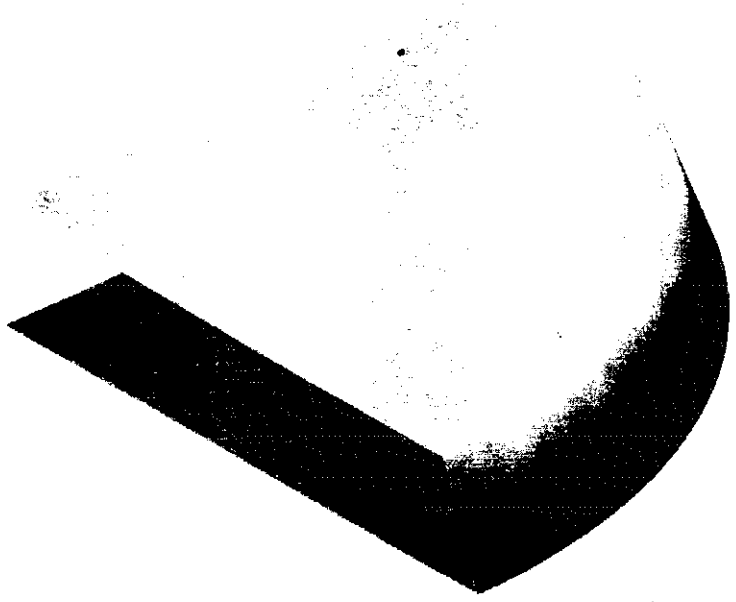

Figure 3. The m.m.e.s. at the instant of collapse.

From Figure 3 it is easy to arrive at the collapse mechanism, which as shown in Figure 4, is characterised by the fact that each section, θ = constant, rotates within its plane by angle φ around the point P of the extrados. As a consequence of this rotation, the point having initial coordinates (r, θ, z) occupies the position $(r + \varphi z, \theta, z + \varphi(R - r))$.

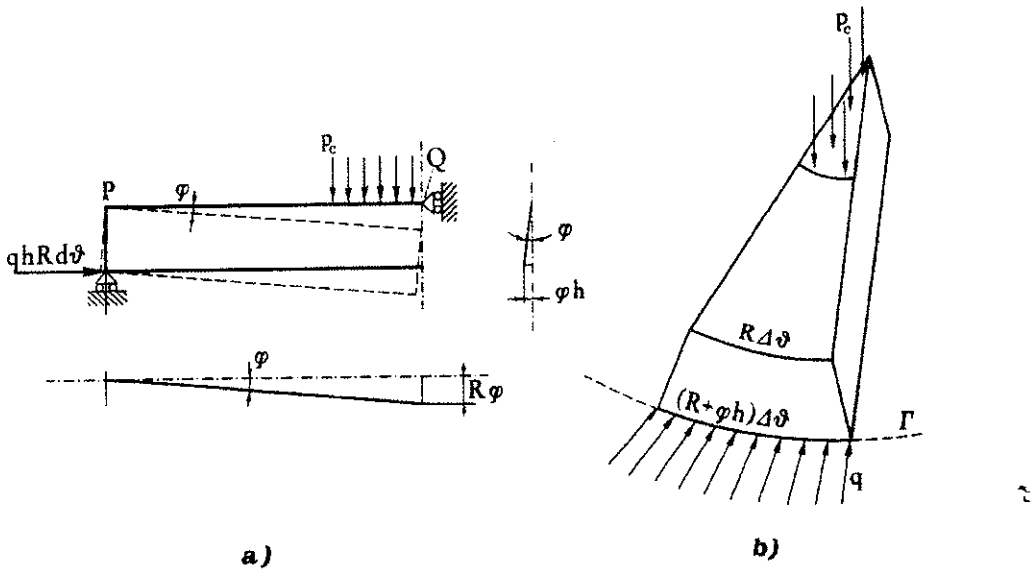

Figure 4. The plate collapse mechanism.

In particular, the points of the generic circumference having its centre on the symmetry axis, radius r_0 and height z_0, are brought onto the circumference with radius $r_0 + \varphi(\frac{1}{2}h + z_0)$, at the level $z_0 + \varphi(R - r_0)$. Therefore the only circumferences whose radii remain unchanged are those of the extrados.

By means of numerical tests similar to those described here, we have verified that the collapse mechanism does not change for values of b less than R or even when a vertical point load is assigned to the centre of the plate.

Once the collapse mechanism is known, it is possible to determine the value p_c of the collapse vertical pressure explicitly. In fact, the work done by p_c for the generic slice of plate with amplitude $\Delta\theta$ is

$$\mathcal{L}_p = \varphi\Delta\theta p_c \int_0^b r\,(R - r)\,dr = \varphi\Delta\theta p_c \frac{b^2(3R - 2b)}{6}, \tag{3.1}$$

whereas the corresponding work done by the lateral pressure is

$$\mathcal{L}_q = -\varphi\Delta\theta qRh^2 . \tag{3.2}$$

Therefore, by requiring the work of the loads at collapse to be zero, from (3.1) and (3.2) we deduce

$$p_c = \frac{6qRh^2}{b^2(3R - 2b)} . \tag{3.3}$$

Relation (3.3) can also be used to arrive at the collapse load F_c for the case of a point load F applied to the center of the plate. In fact, setting $F = \pi b^2 p$, from (3.3) we have

$$F_c = \frac{6\pi qRh^2}{(3R - 2b)} \tag{3.4}$$

and when b goes to zero, we obtain

$$F_c = 2\pi qh^2 ; \tag{3.5}$$

from which it can be seen that F_c, unlike p_c, does not depend on R.

For the numerical example presented in this section, from relation (3.3), with b = R we obtain

$$p_c = \frac{6qh^2}{R^2} = 1.2\ 10^2\ \text{N/m}^2. \tag{3.6}$$

Of course, the value p_s of the pressure p beyond which it is impossible to obtain the plate equilibrium numerically, slightly depends on refinement of the mesh and the entity of final load increments. More precisely, we have verified that, for equal load increments, by using less fine a mesh, we obtain a higher value of p_s. Thus for example, with 1200 and 4800 elements we get $p_s = 1.3\ 10^2$ N/m^2 and $p_s = 1.1\ 10^2$ N/m^2, respectively.

We now intend to furnish an approximate evaluation of eccentricity e_r in the radial direction for $0 \le r \le R$ at the moment of collapse by limiting the treatment to the case of b = R. By imposing the radial force equilibrium of the plate element shown in Figure 5, we obtain

$$\int_0^R n(r)\, dr = qR . \tag{3.7}$$

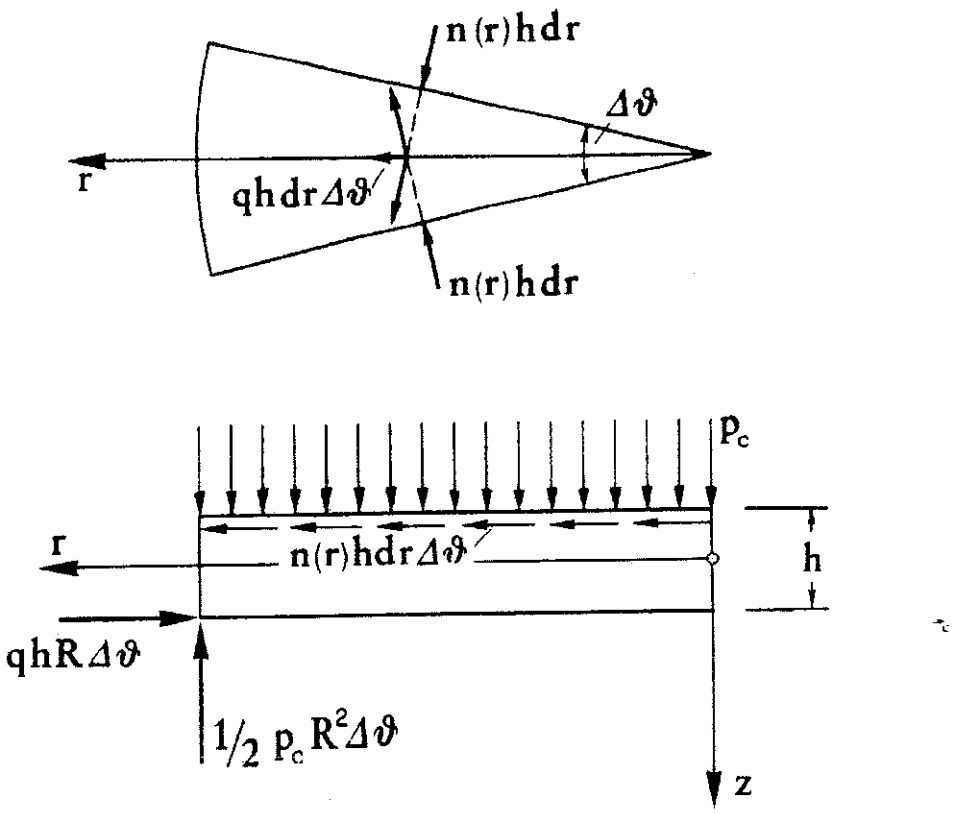

Figure 5. Forces acting on a slice of plate.

Function n(r) is indeterminate, but on the other hand, from the numerical results it seems quite realistic to suppose it to be constant, at least in the case of b = R. Under such an assumption, from (3.7) we obtain n(r) = q and therefore, the circumferential normal force is $N_\theta(r) = -qh$, for $0 \le r \le R$. Since by virtue of the foregoing analysis of the collapse mechanism we have $e_\theta = -\frac{1}{2}h$, in view of (2.10) the circumferential bending moment is

$$M_\theta(r) = \tfrac{1}{2}qh^2 , \quad \text{for} \quad 0 \le r \le R . \tag{3.8}$$

For $M_r(r)$ and $Q(r)$ respectively the radial bending moment and the shear force per unit length (Figure 6), we can write the indefinite equilibrium equation [9]

$$M_r(r) + r\,\frac{dM_r(r)}{dr} - M_\theta(r) + r\,Q(r) = 0 , \tag{3.9}$$

where,

$$Q(r) = \tfrac{1}{2} p_c r , \quad \text{for } 0 \le r \le R . \tag{3.10}$$

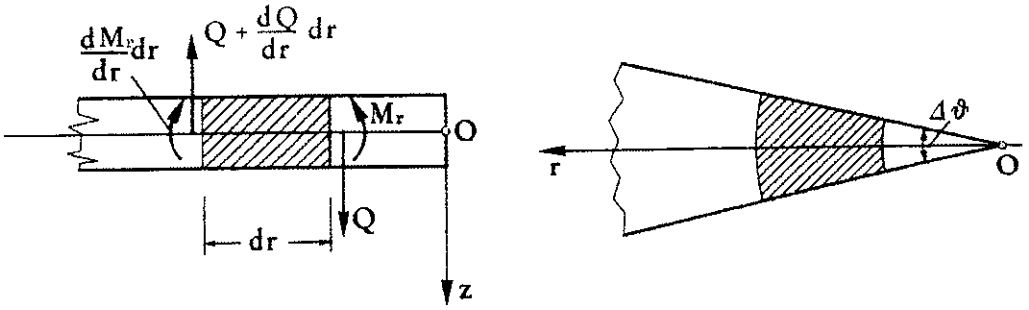

Figure 6. Stress characteristics.

Therefore, in view of (3.8) and (3.10) and from (3.9), we obtain

$$\frac{dM_r(r)}{dr} + \frac{1}{r} M_r(r) = \frac{qh^2}{2r} - \tfrac{1}{2} pr , \qquad \text{for } 0 \le r \le R . \tag{3.11}$$

For $r_0 > 0$ the solution of (3.11) in the interval $[r_0, R]$ is known to be

$$M_r(r) = M_r(r_0) \exp(-A(r)) + \exp(-A(r)) \int_{r_0}^{r} (\frac{qh^2}{2r} - \tfrac{1}{2} pr) \exp(A(s)) \, ds , \tag{3.12}$$

where

$$A(r) = \int_{r_0}^{r} \frac{1}{s} ds = \ln \frac{r}{r_0} . \tag{3.13}$$

Thus we have

$$M_r(r) = M_r(r_0) \frac{r_0}{r} + \tfrac{1}{2} qh^2 (1 - \frac{r_0}{r}) + \frac{p_c}{6} (\frac{r_0^3}{r} - r^2) , \qquad \text{for } r_0 \le r \le R ; \tag{3.14}$$

when r_0 goes to zero, accounting for relation (3.3), with b = R, we obtain

$$M_r(r) = qh^2 \left(\frac{1}{2} - \frac{r^2}{R^2} \right) , \qquad \text{for } 0 \le r \le R . \tag{3.15}$$

By imposing the horizontal force equilibrium of the plate section traced in Figure 6, and taking into account that we have supposed $N_\theta(r) = - qh$, we deduce that the radial normal force N_r is also

constant,

$$N_r(r) = -qh, \quad \text{for } 0 \le r \le R. \tag{3.16}$$

From relations (3.15) and (3.16), we can immediately calculate the eccentricity value in the radial direction,

$$e_r(r) = \frac{M_r(r)}{N_r(r)} = -h\left(\frac{1}{2} - \frac{r^2}{R^2}\right), \quad \text{for } 0 \le r \le R. \tag{3.17}$$

Owing to axial symmetry of both plate and load, equalities $M_{r\theta} = N_{r\theta} = 0$ hold; then in view of (2.10), (3.8), (3.15) and (3.16), for each point (r, θ) of the mean surface of the plate, the value of the eccentricity $e(\alpha)$ relative to the direction which forms angle α with the radial direction is

$$e(\alpha) = -\frac{M_r(r)\cos^2\alpha + M_\theta(r)\sin^2\alpha}{qh} = -h\left(\frac{1}{2} - \frac{r^2}{R^2}\cos^2\alpha\right). \tag{3.18}$$

Figure 7 presents the radial eccentricity e_r as function of r for the considered example: the dotted line has been calculated from the numerically determined stress field, while the continuous line has been obtained using relation (3.17).

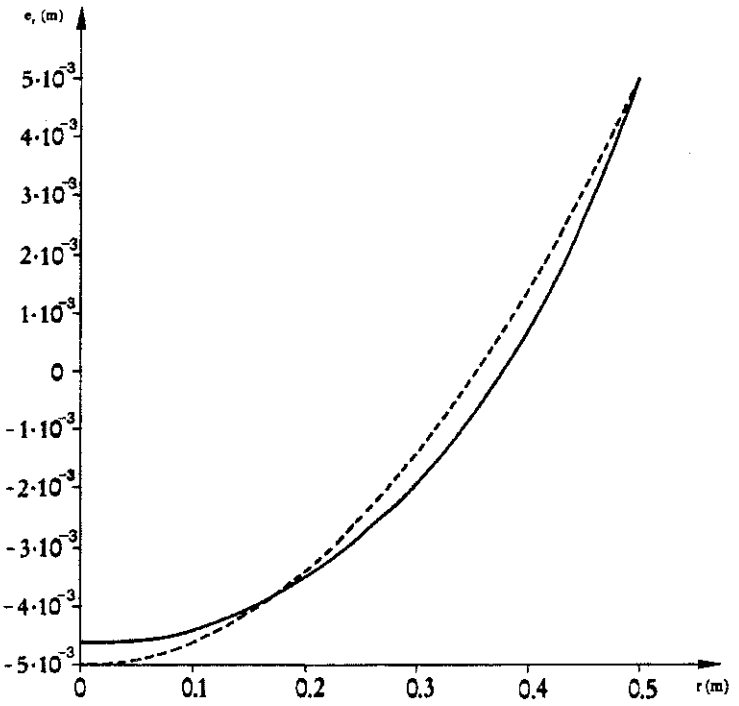

Figure 7. Radial eccentricity e_r vs. r.

4. THE SPHERICAL VAULT

In the spherical reference system $\{O, r, \theta, \varphi\}$, let us consider the spherical vault $\mathcal{V}$ with mean radius R and constant thickness h,

$$\mathcal{V} = \{(r, \theta, \varphi) \mid R - \tfrac{1}{2}h \le r \le R + \tfrac{1}{2}h,\ 0 \le \theta < 2\pi,\ 0 \le \varphi \le \tfrac{1}{2}\pi\}.$$

This is fixed at the springing and subjected to its own weight and a point load P applied at the crown. A vault, with R = 1 m, h = .16 m and specific weight $\gamma = 2.\ 10^4$ N/m^3, has been discretized and analysed by means of the finite element code NOSA.

Figure 8 shows the m.m.e.s. for the vault subjected to its own weight alone. In order to best appreciate the significance of m.m.e.s., Figure 9 presents the circumferential normal force, while Figure 10 depicts the eccentricity in the meridian direction e_φ (continuous line) and circumferential e_θ (dotted line). As proven in Section 2, in the region where the normal force vanishes the two eccentricities coincide. Moreover, as seen towards the end of Section 2, function $|e(\alpha)|$ reaches its maximum value in correspondence to the meridian or the parallel; therefore for the maximum value of the modulus eccentricity we have $\tilde{e} = e_\varphi$, if $|e_\varphi| \ge |e_\theta|$, while $\tilde{e} = e_\theta$, if $|e_\varphi| \le |e_\theta|$.

Figure 8. The m.m.e.s. for the vault subjected to its own weight.

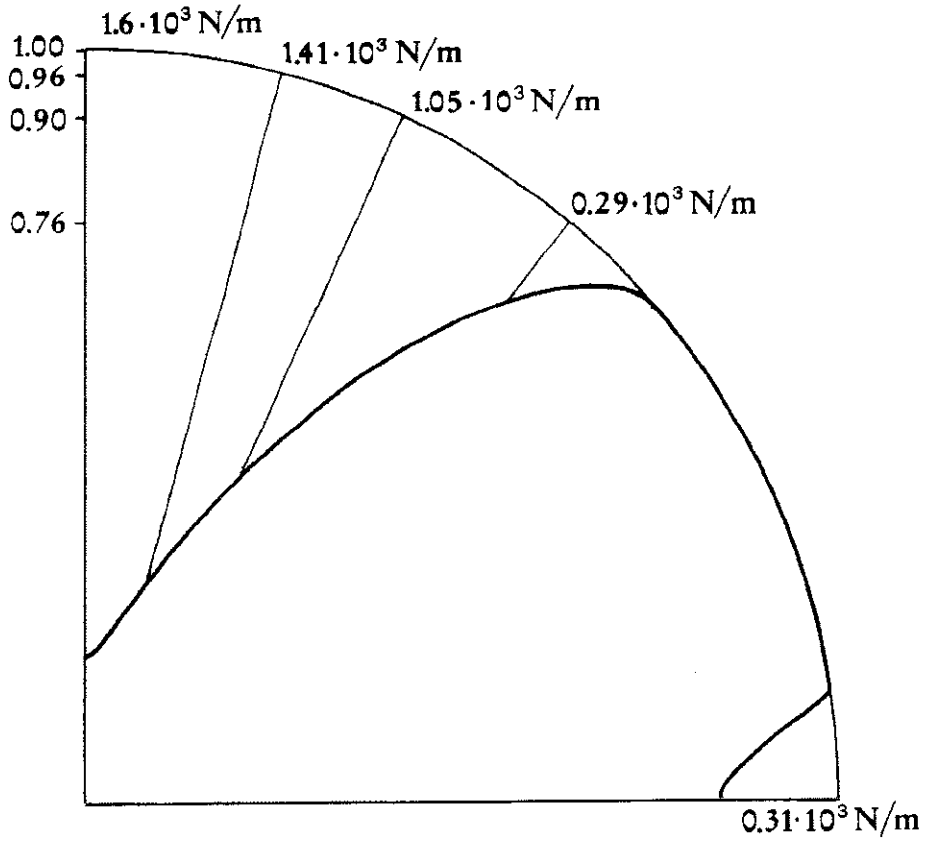

Figure 9. Circumferential normal force for the vault subjected to its own weight.

Then, point load P is increased by increments until reaching the value beyond which it is no longer possible to obtain convergence. The corresponding eccentricity in the meridian direction is shown in Figure 11.

From the numerical analysis it can be seen that for this load value, the circumferential normal force N_θ and the circumferential bending moment M_θ vanish everywhere except at the crown and springings; it therefore seems natural to suppose that the collapse of the vault is due to an "orange slice" mechanism, namely, that slices of infinitesimal size behave like arches. Once the collapse mechanism is known, the value P_c of the load at collapse can be determined through simple considerations of rigid-body kinematics, as described in [2]. For the case at hand, proceeding in this way we obtain $P_c = 6230$ N.

Now we intend to determine the m.m.e.s. explicitly. Since the circumferential normal force is nil, as proven in Section 2, the eccentricity throughout is independent of the choice of direction in the plane tangent to the mean surface; therefore the m.m.e.s. is completely characterised by the eccentricity corresponding to the meridian direction.

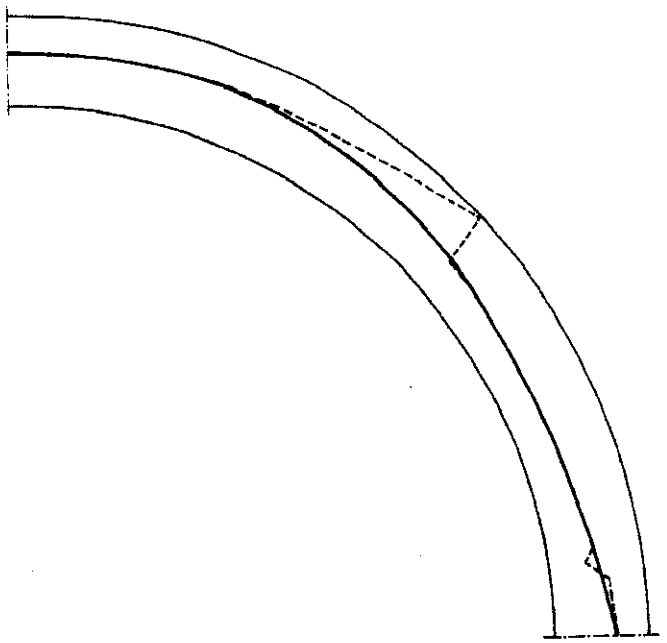

Figure 10. Eccentricities e_φ and e_θ for the vault subjected to its own weight.

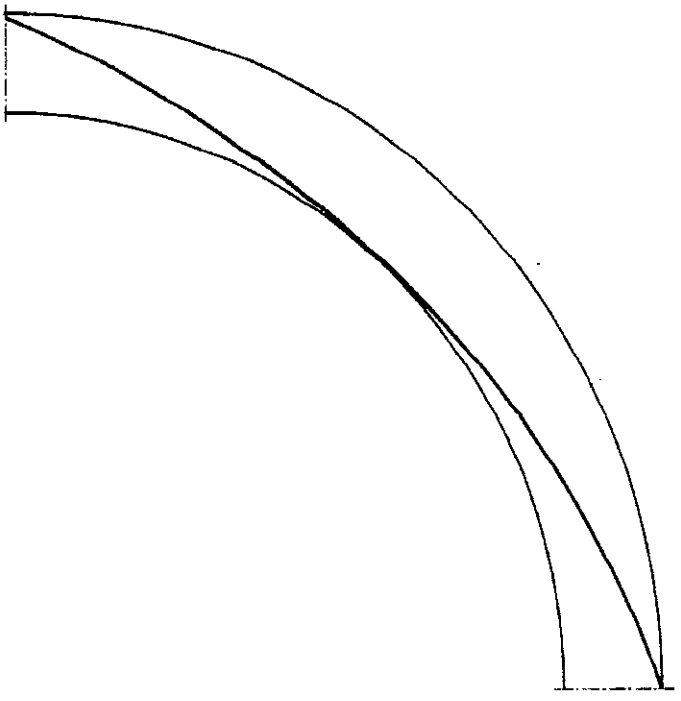

Figure 11. Eccentricity e_φ for the vault at collapse.

Denoting q as the weight of the vault per unit area, N and M as the meridian normal force and bending moment, respectively, and Q as the shear, we can write the indefinite equilibrium equations [7] for $N_\theta = 0$, $M_\theta = 0$,

$$\frac{dN(\varphi)}{d\varphi}\sin\varphi + N(\varphi)\cos\varphi - Q(\varphi)\sin\varphi + R\,q\sin^2\varphi = 0\,, \tag{4.1}$$

$$N(\varphi)\sin\varphi + \frac{dQ(\varphi)}{d\varphi}\sin\varphi + Q(\varphi)\cos\varphi + R\,q\sin\varphi\cos\varphi = 0\,, \tag{4.2}$$

$$\frac{dM(\varphi)}{d\varphi}\sin\varphi + M(\varphi)\cos\varphi - Q(\varphi)\,R\sin\varphi = 0\,. \tag{4.3}$$

Moreover, by imposing the vertical force equilibrium of the spherical bowl with amplitude φ, we obtain

$$2\pi R\,N(\varphi)\sin^2\varphi + 2\pi R\,Q(\varphi)\cos\varphi\sin\varphi + T(\varphi) = 0 \tag{4.4}$$

where, for P_c the collapse value of point load P,

$$T(\varphi) = 2\pi R^2 q(1 - \cos\varphi) + P_c \tag{4.5}$$

is the total load acting on the spherical bowl. Taking $Q(\varphi)$ from (4.4) and substituting it into (4.1) we get

$$\frac{dN(\varphi)}{d\varphi}\sin\varphi + N(\varphi)\cos\varphi + \frac{2\pi R\,N(\varphi)\sin^2\varphi + T(\varphi)}{2\pi R\cos\varphi} + R\,q\sin^2\varphi = 0\,, \tag{4.6}$$

from which

$$\frac{dN(\varphi)}{d\varphi} + \frac{N(\varphi)}{\sin\varphi\cos\varphi} = \frac{R\,q(\cos\varphi - \cos\varphi\sin^2\varphi - 1 - p_c)}{\sin\varphi\cos\varphi}\,, \tag{4.7}$$

where we have put

$$p_c = \frac{P_c}{2\pi R^2 q}\,. \tag{4.8}$$

For each $\varphi_0 > 0$, the solution of (4.7) in the interval $[\varphi_0, \frac{1}{2}\pi]$ is

$$N(\varphi) = N(\varphi_0)\,\frac{\tan\varphi_0}{\tan\varphi} + \frac{R\,q}{\tan\varphi}\{\sin\varphi - \sin\varphi_0 - (1 + p_c)(\tan\varphi - \tan\varphi_0)\}\,, \tag{4.9}$$

which has a singularity at $\varphi = 0$. On the other hand, for each $\varphi_0 > 0$, we take the vault lacking the spherical bowl of amplitude φ_0 and extract a slice of amplitude $\Delta\theta$; imposing the horizontal force equilibrium of this latter, we obtain

$$R\,\Delta\theta\,\{N(\varphi_0)\cos\varphi_0\,\sin\varphi_0 - Q(\varphi_0)\sin^2\varphi_0 + Q(\tfrac{1}{2}\pi)\} = 0\,. \tag{4.10}$$

From this relation we deduce that, when φ_0 tends towards zero, $N(\varphi_0)\sin\varphi_0$ goes to $-Q(\frac{1}{2}\pi)$; therefore the desired solution of (4.7) in the interval $(0, \frac{1}{2}\pi]$ is

$$N(\varphi) = -\frac{Q(\tfrac{1}{2}\pi)\cos\varphi}{\sin\varphi} + R\,q(\cos\varphi - 1 - p_c)\,. \tag{4.11}$$

From the previous relation, with the help of (4.4) and (4.5) we can easily deduce the expression for shear

$$Q(\varphi) = Q(\tfrac{1}{2}\pi) - \frac{R\,q\,(1 + p_c - \cos\varphi)\cos\varphi}{\sin\varphi}\,. \tag{4.12}$$

As $Q(\varphi)$ is known, it is now possible to integrate equation (4.3), by following a procedure similar to that used for determining $N(\varphi)$. In this way we obtain

$$M(\varphi) = \frac{1}{\sin\varphi}\{M(\tfrac{1}{2}\pi) - R\,Q(\tfrac{1}{2}\pi)\cos\varphi + \\ + q\,R^2[\tfrac{1}{2}\varphi + \tfrac{1}{4}\sin 2\varphi - (1 + p_c)\sin\varphi + 1 + p_c - \tfrac{1}{4}\pi]\}\,. \tag{4.13}$$

The two constants $Q(\frac{1}{2}\pi)$ and $M(\frac{1}{2}\pi)$ can be easily determined by assuming that at collapse two hinges form at the extrados, the former at the crown and the latter at the springing. Then, recalling that h is the thickness of the vault, we have

$$e(0) = \frac{M(0)}{N(0)} = -\frac{h}{2}\,, \qquad e(\tfrac{1}{2}\pi) = \frac{M(\tfrac{1}{2}\pi)}{N(\tfrac{1}{2}\pi)} = -\frac{h}{2}\,. \tag{4.14}$$

Using these relations and placing

$$t = \frac{h}{2R}\,, \tag{4.15}$$

we obtain

$$Q(\tfrac{1}{2}\pi) = q\,R\,(1 + p_c + \frac{\pi}{4(1+t)})\,, \tag{4.16}$$

$$M(\tfrac{1}{2}\pi) = q\,R^2 t\,(1 + p_c)\,, \tag{4.17}$$

which, in turn, enables us to finally arrive at the expressions for the normal force and bending moment at the instant of collapse. In fact, from (4.11), (4.13), (4.16) and (4.17), we obtain

$$N(\varphi) = -\frac{q\,R}{\sin\varphi}\{(1 + p_c - \frac{\pi}{4(1+t)})\cos\varphi + (1 + p_c - \cos\varphi)\sin\varphi\}\,, \tag{4.18}$$

$$M(\varphi) = \frac{q\,R^2}{\sin\varphi}\{t\,(1 + p_c) - (1 + p_c - \frac{\pi}{4(1+t)})\cos\varphi +$$

$$+ \tfrac{1}{4}(2\varphi + \sin 2\varphi) - (1 + p_c)\sin\varphi + (1 + p_c - \tfrac{1}{4}\pi)\}\,. \tag{4.19}$$

Therefore, the eccentricity, which as already mentioned depends only on the angle φ, is

$$e(\varphi) = \frac{M(\varphi)}{N(\varphi)} =$$

$$= -R\,\frac{(t - \sin\varphi)(1 + p_c) - (1 + p_c - \frac{\pi}{4(1+t)})\cos\varphi + \tfrac{1}{4}(2\varphi + \sin 2\varphi) + 1 + p_c - \tfrac{1}{4}\pi}{(1 + p_c - \frac{\pi}{4(1+t)})\cos\varphi + (1 + p_c - \cos\varphi)\sin\varphi}\,. \tag{4.20}$$

In Figure 12 the eccentricity derived from the stress field calculated numerically for the instant of collapse (dotted line) and shown in Figure 11 is compared to the eccentricity obtained from relation (4.20) (continuous line).

It is interesting to point out that the collapse load can be determined with the help of (4.20) by observing that it coincides with the maximum value of p_c for which relation $|e(\varphi)| \le \tfrac{1}{2}h$ holds for all $\varphi \in [0, \tfrac{1}{2}\pi]$; in the current example we obtain $p_c = .31$, which of course corresponds to the value of $P_c = 6230$ N, determined through rigid-body kinematics.

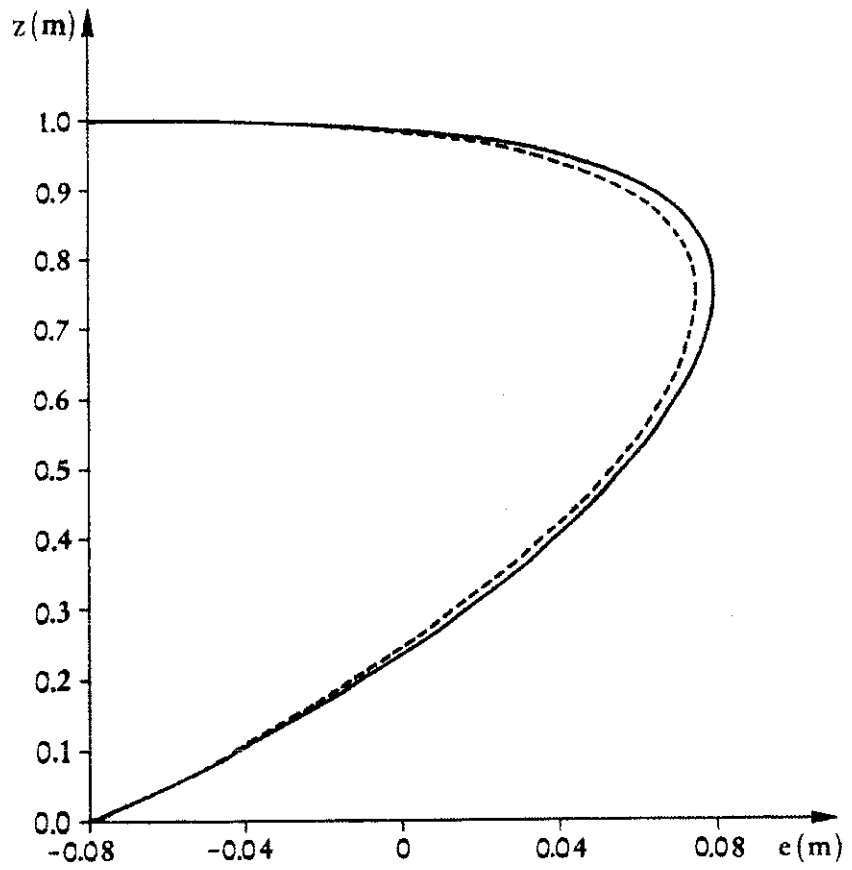

Figure 12. Eccentricity e vs. z = R cos φ at collapse.

5. THE BAPTISTERY OF VOLTERRA CATHEDRAL

The Romanesque baptistery in Volterra, dating from the X Century, has an octagonal floor plan (Figures. 13 a and 13 b).

The current dome crowning the baptistery is not the original roof. The original had probably another form quite unlike today's structure. In about the year 1427, the current cupola of the baptistery was constructed in brick masonry of thickness varying from 0.6 m at the keystone to 0.9 m at the springing [8]. It has since undergone cracking on the vault itself, as well as on the walls of the baptistery octagon, and these latter have consequently been raised by 2.75 m. Finally, in 1930 restoration and reinforcement was carried out which included, among other measures, the application to the cupola of two chains of cross-section .04 x .07 m^2 and .03 x.06 m^2 at distances of 1.2 m and 3.4 m from the springing, respectively (Figure 13 c). Another chain was placed on the octagon walls just above the upper windows. The positioning of the chains was decided upon

by considering the material to be linear elastic and applying the calculation procedures described in [9]. More precisely, a 22.5° wedge of arch was considered and subdivided into 13 blocks, each 1.2 m in length. It was assumed that the force normal to the lateral face of the blocks was exerted upon the baricenters of the block faces themselves. Furthermore, the line of thrust was constrained to pass through the baricenter of all the blocks. Using this procedure, it was deduced that the circumferential compressive force increased from the crown down to a certain height, after which it dwindles to zero at the parallel at 24° from the springing plane. It was therefore decided to chain the cupola at this same parallel and place another near the springing.

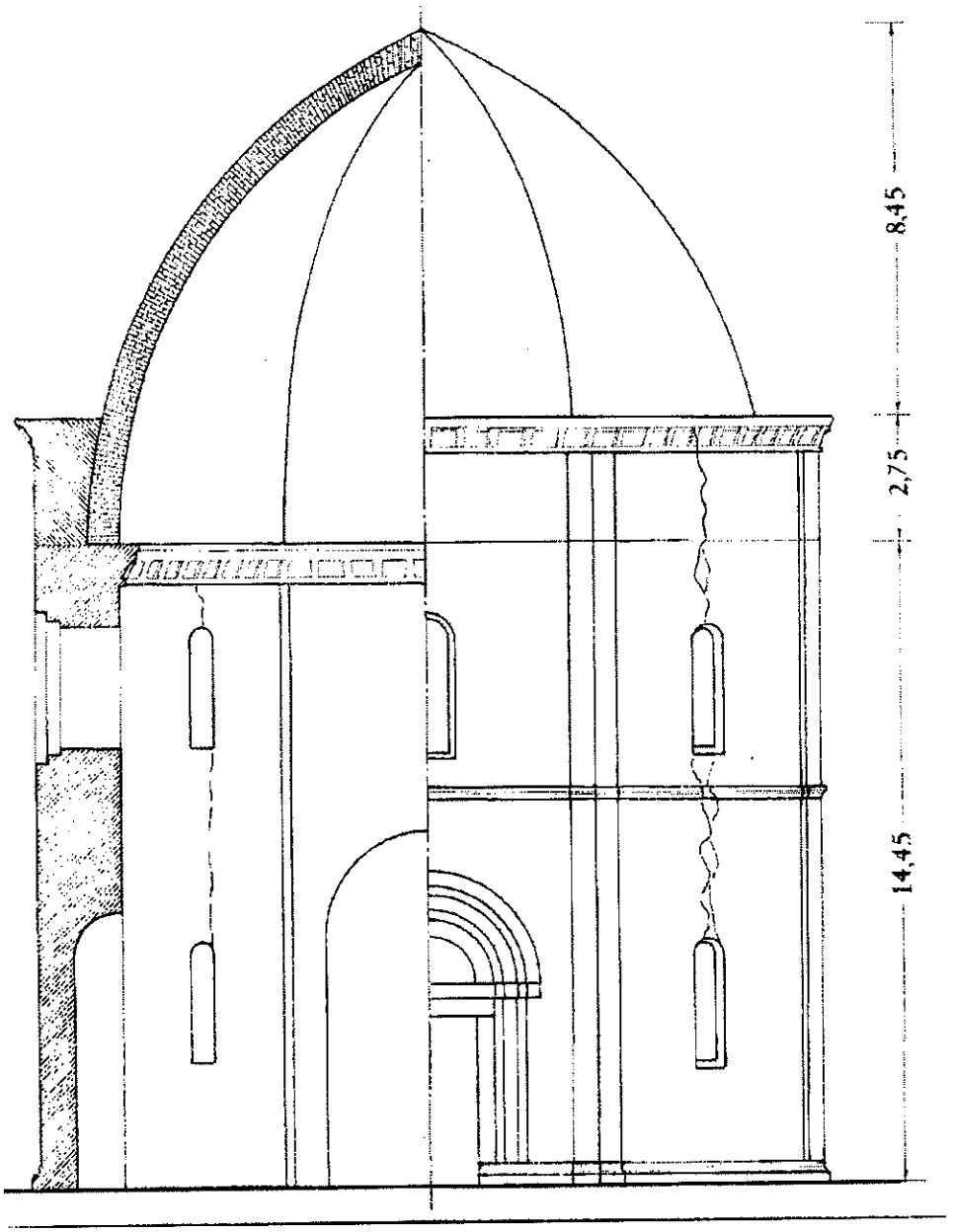

Figure 13 a. View of the baptistery.

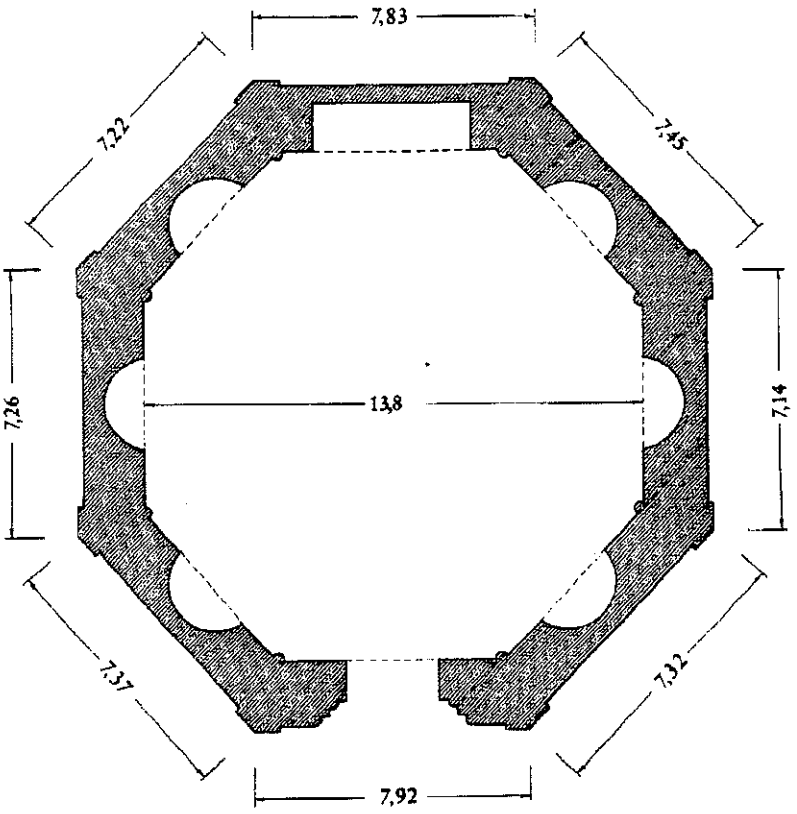

Figure 13 b. Baptistery floor-plan.

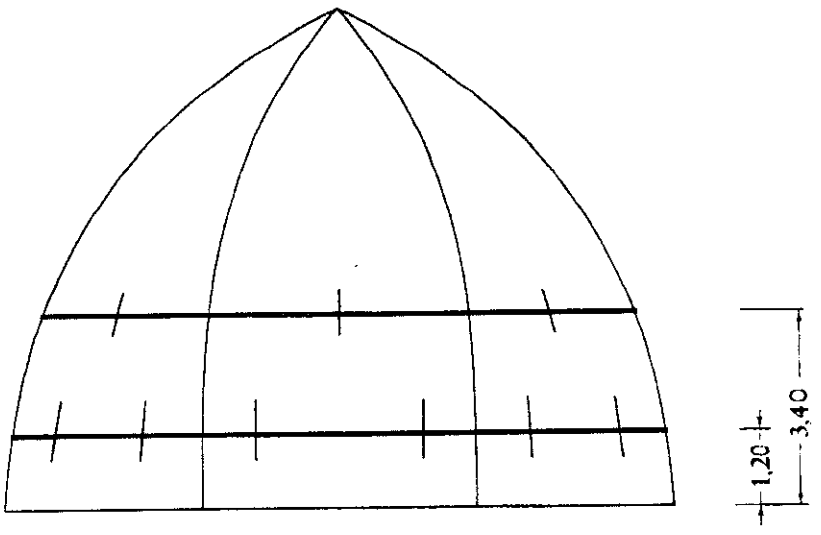

Figure 13 c. View of the baptistery vault with chains.

The baptistery is currently undergoing restoration work which includes refacing of the vault covering, as it has been damaged by rainwater seepage. The baptistery has been studied with the NOSA code, assuming that the material does not support tension.

In a first treatment, only the chain on the octagon walls was considered. Figure 1 presents the line of thrust corresponding to one vaulting rib. The minimum distance of the line of thrust from the intrados is 0.22 m, at a height of 3.12 m, while the line's minimum distance from the extrados is 0.12 m at a height of 8.64 m.

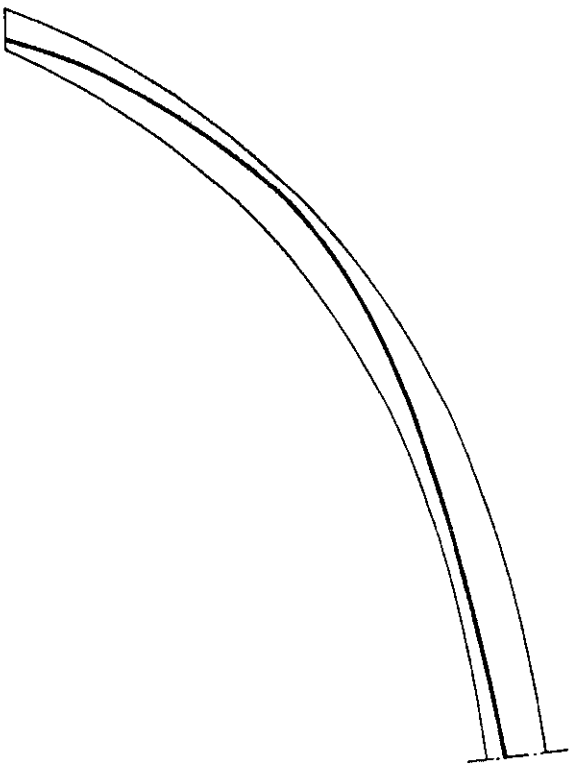

Figure 14. Line of thrust in a vault rib without chains.

The analysis was then repeated to account for the presence of the two chains reinforcing the vault itself. The relative line of thrust, depicted in figure 15, is almost entirely contained within the dome's middle third. The sustaining effect of the chains is therefore evident. Figure 16 shows the pattern of the normal circumferential force along a single vault rib.

The tensile forces on the chains reach their maximums in correspondence to the apothem, where their values are 5548 N and 10984 N for the upper and lower chain, respectively. The chain reinforcing the baptistery octagon walls experiences a maximum traction of 19400 N near the window, precisely in the area where cracking has occurred. The importance of this chain can be deduced from the fact that without it, tensile forces on the two vault chains would reach levels of 25960 N and 49990 N, respectively for the upper and lower chains.

A further determination was carried out with the aim of checking the results obtained by means of the method proposed in [9]. This analysis consisted of numerically calculating the stress in the

dome under the assumption that the material is linear elastic. Figure 17 presents the distribution of the normal circumferential force along a vault rib. It can be seen that this value is negative solely up to an angle of 40°, as measured from the springing; which corresponds to a height of 5.2 m. On the basis of these results, analysis of the baptistery vault was performed once again under the assumption that the upper chain were placed at a height of 5.2 m, rather than the actual 3.4 m.

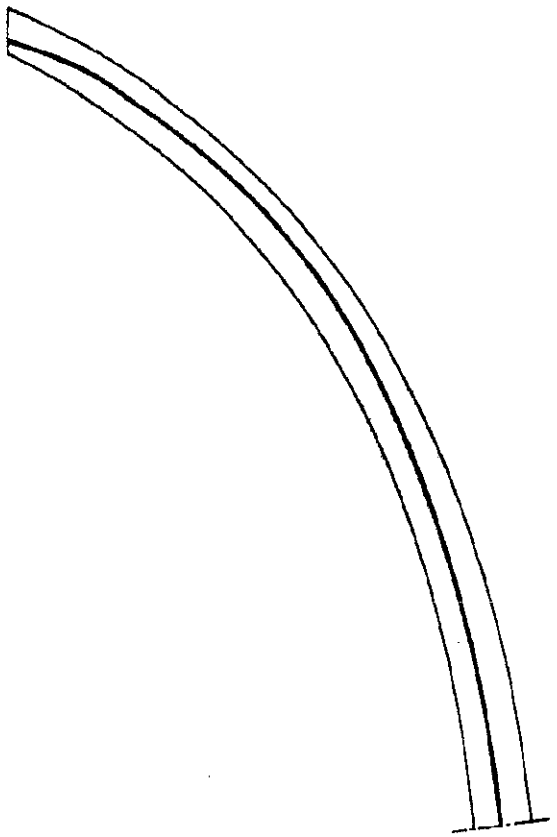

Figure 15. Line of thrust in a vault rib in the presence of two chains.

For the sake of comparison, figure 18 shows the results calculated under the foregoing assumptions (dotted line) together with those obtained using the actual placement of the chains (continuous line). It can be seen that, despite inaccurate assessment of the normal force, the placement of the chains turns out to be quite good. Then, it should be emphasized that the criterion used in choosing the parallel at which to position the chain, (i.e. where the normal force falls to zero) is not the most appropriate. A more suitable procedure would instead be to chain at the parallel corresponding to the exertion point of the resultant of tensile forces as calculated through linear elastic analysis.

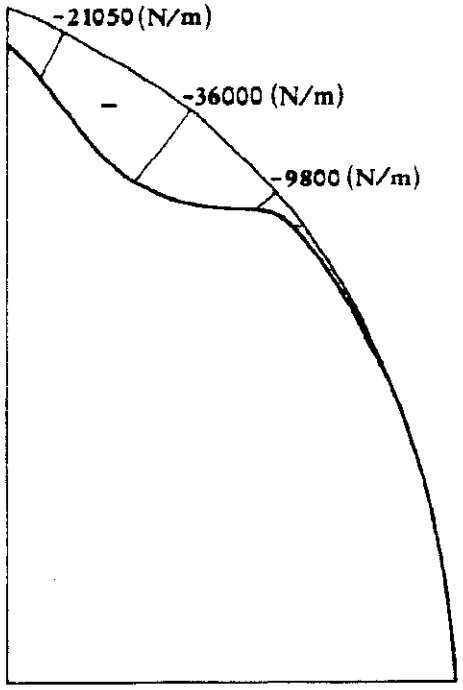

Figure 16. The normal circumferential force in a vault rib in the presence of two chains.

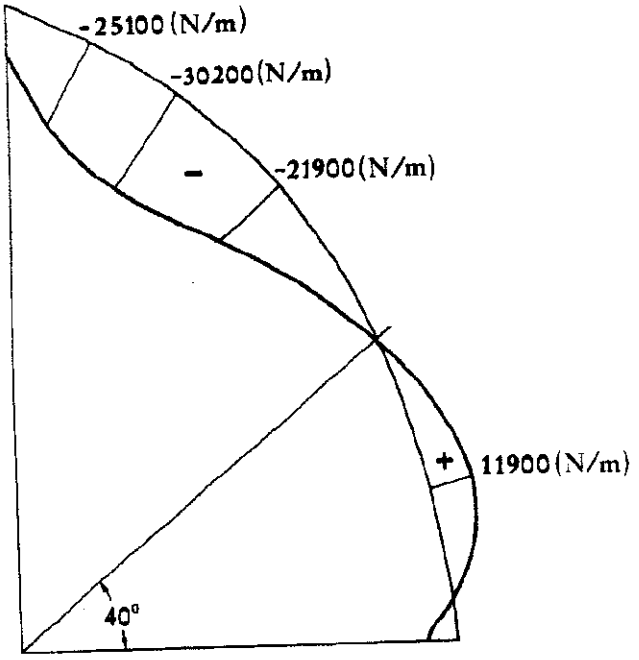

Figure 17. The normal circumferential force along a vault rib assuming the material to be linear elastic.

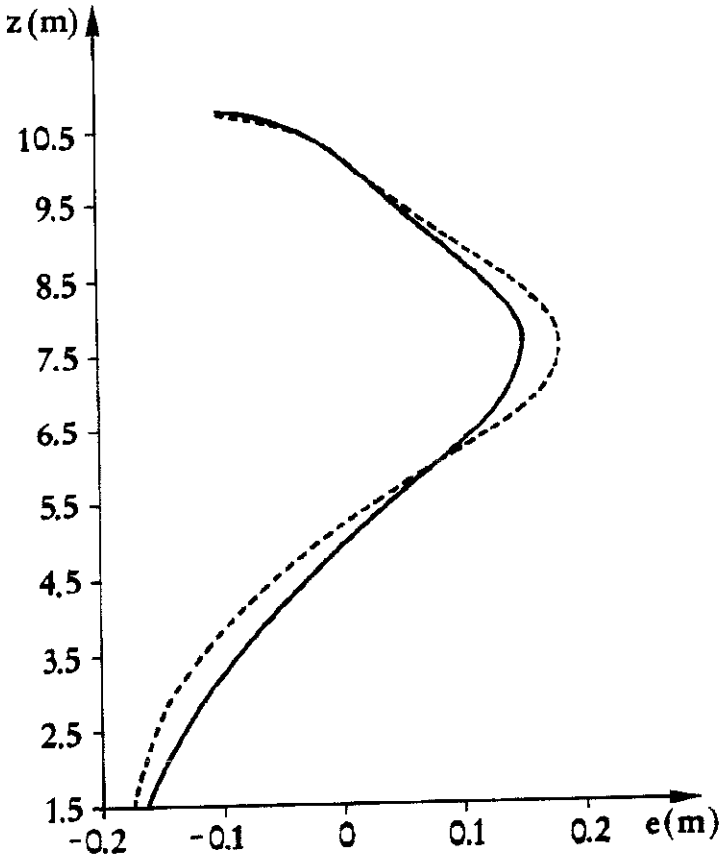

Figure 18. Eccentricity along a vault rib as a function of height.

Acknowledgments: We wish to thank Salvatore Di Pasquale for his useful suggestions and the Sprintendenza ai Monumenti e Gallerie di Pisa for having so kindly provided documentation on the Volterra baptistery.

REFERENCES

1. M. Lucchesi, C. Padovani, A. Pagni, A numerical method for solving equilibrium problems of masonry-like solids. *Meccanica* 29, 175-193 (1994).
2. M. Lucchesi, C. Padovani, G. Pasquinelli, On the numerical solution of equilibrium problems of elastic solids with bounded tensile strength. To appear in *Comp. Meth. Appl. Mech. Eng.* (1994).
3. M. Lucchesi, C. Padovani, N. Zani, Masonry-like materials with bounded compressive strength. To appear in *Int. J. Sol. Struct.* (1995).

4. The Finite Element Code NOSA. User's Manual. Compiled by the Mechanics of Materials and Structures" Team of CNUCE. Technical Report ZC 236-94 (1994).
5. P. Guidotti, A non conforming thin shell. Quaderno de "La Ricerca Scientifica" del C.N.R. **115**, 95-115, (1986).
6. J. Heyman, *The masonry arch.* J. Wiley & Sons, 1982.
7. S. P. Timoshenko, S. Woinowsky-Krieger, *Theory of plates and shells.* Mc-Graw-Hill Int. Ed., 1987.
8. Leoncini, G. (1869). *Illustrazione sulla cattedrale di Volterra.* Tipografia Sordo-muti di Luigi Lazzari.
9. Guidi, C. (1913). *Lezioni sulla scienza delle costruzioni.* Politecnico di Torino.